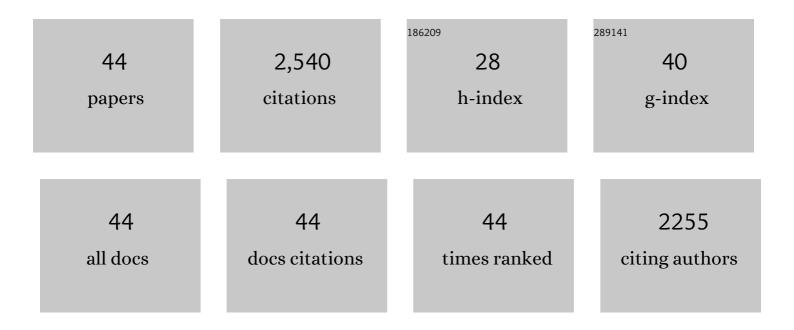
## List of Publications by Year in descending order

Source: https://exaly.com/author-pdf/11331981/publications.pdf Version: 2024-02-01



#	Article	IF	CITATIONS
1	Highly efficient adsorption of strontium ions by carbonated mesoporous TiO2. Journal of Molecular Liquids, 2019, 285, 742-753.	2.3	204
2	Structural, Optical, and Magnetic Properties of Zn-Doped CoFe2O4 Nanoparticles. Nanoscale Research Letters, 2017, 12, 141.	3.1	193
3	Adsorption of textile dye using para-aminobenzoic acid modified activated carbon: Kinetic and equilibrium studies. Journal of Molecular Liquids, 2019, 296, 112075.	2.3	168
4	Removal of caffeine, nicotine and amoxicillin from (waste)waters by various adsorbents. A review. Journal of Environmental Management, 2020, 261, 110236.	3.8	152
5	Synthesis, morphology, crystallite size and adsorption properties of nanostructured Mg–Zn ferrites with enhanced porous structure. Journal of Alloys and Compounds, 2020, 819, 152945.	2.8	118
6	Halloysite nanotubes and halloysite-based composites for environmental and biomedical applications. Journal of Molecular Liquids, 2020, 309, 113077.	2.3	112
7	Spinel Ferrite Nanoparticles: Synthesis, Crystal Structure, Properties, and Perspective Applications. Springer Proceedings in Physics, 2017, , 305-325.	0.1	110
8	Facile microwave-assisted green synthesis of NiO nanoparticles from <i>Andrographis paniculata</i> leaf extract and evaluation of their photocatalytic and anticancer activities. Molecular Crystals and Liquid Crystals, 2018, 673, 70-80.	0.4	98
9	Adsorptive removal of toxic Methylene Blue and Acid Orange 7 dyes from aqueous medium using cobalt-zinc ferrite nanoadsorbents. , 0, 150, 374-385.		94
10	A review on removal of uranium(VI) ions using titanium dioxide based sorbents. Journal of Molecular Liquids, 2019, 293, 111563.	2.3	84
11	Green synthesis, structure, cations distribution and bonding characteristics of superparamagnetic cobalt-zinc ferrites nanoparticles for Pb(II) adsorption and magnetic hyperthermia applications. Journal of Molecular Liquids, 2021, 328, 115375.	2.3	72
12	Elastic properties and antistructural modeling for Nickel-Zinc ferrite-aluminates. Materials Chemistry and Physics, 2018, 207, 534-541.	2.0	71
13	Effect of Zn addition on structural, magnetic properties and anti-structural modeling of magnesium-nickel nano ferrites. Materials Chemistry and Physics, 2019, 229, 78-86.	2.0	64
14	Green Synthesis of Metal and Metal Oxide Nanoparticles: Principles of Green Chemistry and Raw Materials. Magnetochemistry, 2021, 7, 145.	1.0	64
15	Adsorption of Sr(II) ions and salicylic acid onto magnetic magnesium-zinc ferrites: isotherms and kinetic studies. Environmental Science and Pollution Research, 2020, 27, 26681-26693.	2.7	59
16	Microwave-assisted green synthesis of SnO <sub>2</sub> nanoparticles and their optical and photocatalytic properties. Molecular Crystals and Liquid Crystals, 2018, 671, 17-23.	0.4	58
17	Effects of chemosorbed arsenate groups on the mesoporous titania morphology and enhanced adsorption properties towards Sr(II) cations. Journal of Molecular Liquids, 2019, 282, 587-597.	2.3	58

<sup>18</sup> Synthesis and magnetic properties of spinel Zn1â<sup>°</sup>xNixFe2O4 (0.0â€â‰**å**€¯xâ€â‰**å**€¯1.0) nanoparticles synthesized by microwave combustion method. Journal of Magnetism and Magnetic Materials, 2019, 471, 192-199. <sup>56</sup>

#	Article	IF	CITATIONS
19	Structure, morphology and adsorption properties of titania shell immobilized onto cobalt ferrite nanoparticle core. Journal of Molecular Liquids, 2020, 297, 111757.	2.3	55
20	Spinel cobalt(II) ferrite-chromites as catalysts for H2O2 decomposition: Synthesis, morphology, cation distribution and antistructure model of active centers formation. Ceramics International, 2020, 46, 27517-27530.	2.3	54
21	Magnesium-zinc ferrites as magnetic adsorbents for Cr(VI) and Ni(II) ions removal: Cation distribution and antistructure modeling. Chemosphere, 2021, 270, 129414.	4.2	54
22	Dual control on structure and magnetic properties of Mg ferrite: Role of swift heavy ion irradiation. Journal of Magnetism and Magnetic Materials, 2019, 471, 521-528.	1.0	50
23	Synthesis of hierarchical structured rare earth metal–doped Co3O4 by polymer combustion method for high performance electrochemical supercapacitor electrode materials. Ionics, 2020, 26, 2051-2061.	1.2	47
24	Structure–redox reactivity relationships in Co <sub>1â"x</sub> Zn <sub>x</sub> Fe <sub>2</sub> O <sub>4</sub> : the role of stoichiometry. New Journal of Chemistry, 2019, 43, 3038-3049.	1.4	46
25	Inversion degree, morphology and colorimetric parameters of cobalt aluminate nanopigments depending on reductant type in solution combustion synthesis. Ceramics International, 2020, 46, 14674-14685.	2.3	45
26	Photovoltaic device performance of pure, manganese (Mn <sup>2+</sup> ) doped and irradiated CuInSe <sub>2</sub> thin films. New Journal of Chemistry, 2018, 42, 11642-11652.	1.4	40
27	Green synthesis of cobalt ferrite nanoparticles using <i>Cydonia oblonga</i> extract: structural and mössbauer studies. Molecular Crystals and Liquid Crystals, 2018, 672, 54-66.	0.4	38
28	Adsorption of Sr(II) cations onto phosphated mesoporous titanium dioxide: Mechanism, isotherm and kinetics studies. Journal of Environmental Chemical Engineering, 2019, 7, 103430.	3.3	36
29	Physicochemical and electrochemical properties of Gd3+-doped ZnSe thin films fabricated by single-step electrochemical deposition process. Journal of Solid State Electrochemistry, 2018, 22, 1197-1207.	1.2	33
30	Comparative study of structural, optical and electrical properties of electrochemically deposited Eu, Sm and Gd doped ZnSe thin films. Journal of Materials Science: Materials in Electronics, 2018, 29, 5638-5648.	1.1	30
31	La-doped Ni <sub>0.5</sub> Co <sub>0.5</sub> Fe <sub>2</sub> O <sub>4</sub> nanoparticles: effect of cobalt precursors on structure and morphology. Molecular Crystals and Liquid Crystals, 2018, 674, 110-119.	0.4	23
32	Green and Ecofriendly Materials for the Remediation of Inorganic and Organic Pollutants in Water. , 2019, , 69-110.		22
33	Photocatalytic degradation of dyes using rutile TiO2 synthesized by reverse micelle and low temperature methods: real-time monitoring of the degradation kinetics. Journal of Molecular Liquids, 2021, 342, 117407.	2.3	22
34	Eco-friendly synthesis of cobalt-zinc ferrites using quince extract for adsorption and catalytic applications: An approach towards environmental remediation. Chemosphere, 2022, 294, 133565.	4.2	22
35	Catalytic and Photocatalytic Properties of Oxide Spinels. , 2019, , 1701-1750.		16
36	Optimization of TiO2-P25 photocatalyst dose and H2O2 concentration for advanced photo-oxidation using smartphone-based colorimetry. Water Science and Technology, 2021, 84, 469-483.	1.2	15

#	Article	IF	CITATIONS
37	Green synthesis of cobalt ferrite using grape extract: the impact of cation distribution and inversion degree on the catalytic activity in the decomposition of hydrogen peroxide. Emergent Materials, 2022, 5, 89-103.	3.2	14
38	Cr content-dependent modification of structural, magnetic properties and bandgap in green synthesized Co–Cr nano-ferrites. Molecular Crystals and Liquid Crystals, 2020, 699, 39-50.	0.4	11
39	Removal of Congo Red dye, polar and non-polar compounds from aqueous solution using magnesium aluminate nanoparticles. Materials Today: Proceedings, 2021, 35, 518-522.	0.9	9
40	Green Synthesis of Magnetic Spinel Nanoparticles. Springer Proceedings in Physics, 2019, , 389-398.	0.1	8
41	Optimal H2O2 concentration in advanced oxidation over titanium dioxide photocatalyst. Physics and Chemistry of Solid State, 2021, 22, 73-79.	0.3	4
42	Green synthesis of zinc ferrite. Molecular Crystals and Liquid Crystals, 2021, 719, 45-52.	0.4	4
43	Catalytic and Photocatalytic Properties of Oxide Spinels. , 2018, , 1-50.		4
44	Catalytic activity of magnetite and its magnetic heating properties. Materials Today: Proceedings, 2022, 62, 5805-5811.	0.9	3